Available online at www.sciencedirect.com
ScienceDirect
Applied Surface Science 254 (2007) 1399–1404
applied surface science
www.elsevier.com/locate/apsusc

Catalytic behaviors of ruthenium dioxide films deposited on ferroelectrics substrates, by spin coating process

M. Khachane [a,b], P. Nowakowski [b], S. Villain [b], J.R. Gavarri [b,*], Ch. Muller [b], M. Elaatmani [a], A. Outzourhite [c], I. Luk'yanchuk [d], A. Zegzouti [a], M. Daoud [a]

[a] *Laboratoire de Chimie du Solide Minéral, département de chimie, Faculté des Sciences Semlalia, Université Cadi Ayyad BP: 2390, Marrakech, Morocco*

[b] *Laboratoire Matériaux & Microélectronique de Provence, – UMR CNRS 6137, Université du Sud Toulon Var – BP 20132, F-83957 La Garde, France*

[c] *Laboratoire de physique du Solide et couches minces, département de physique, Faculté des Sciences Semlalia, Université Cadi Ayyad BP: 2390, Marrakech, Morocco*

[d] *Laboratoire de Physique de la Matière Condensée, Université Picardie Jules Vernes Amiens, France*

Received 22 May 2007; received in revised form 28 June 2007; accepted 28 June 2007
Available online 4 July 2007

Abstract

Catalytic ruthenium dioxide films were deposited by spin-coating process on ferroelectric films mainly constituted of $SrBi_2Ta_2O_9$ (SBT) and $Ba_2NaNb_5O_{15}$ (BNN) phases. After thermal treatment under air, these ferroelectric–catalytic systems were characterized by X-ray diffraction and scanning electron microscopy (SEM). SEM images showed that RuO_2 film morphology depended on substrate nature. A study of CH_4 conversion into CO_2 and H_2O was carried out using these catalytic–ferroelectric multilayers: the conversion was analyzed from Fourier transform infrared (FTIR) spectroscopy, at various temperatures. Improved catalytic properties were observed for RuO_2 films deposited on BNN oxide layer.

PACS : 81.20.Fw; 81.15.-z; 68.55.–a; 81.15.Aa; 82.45.Jn; 82.65.-s; 81.16.Hc; 82.80.Gk; 68.65.Ac

Keywords: Ruthenium dioxide; Sol–gel processing; Multilayer; Infrared spectroscopy; Catalytic measurements

1. Introduction

Ruthenium dioxide (RuO_2) crystallizes in a tetragonal rutile-type structure (space group $P4_2/m\ n\ m$, cell parameters: $a = 450.9$, $c = 310.87$ pm) and presents a metallic conductivity in a wide temperature range, arising from the partially filled Ru 4d states [1,2]. In addition, it presents a high thermal stability under air, namely up to 700 °C, with a low electron resistivity. The high interest of this oxide resides in the fact that it might be involved in many attractive applications [3]. It might be used as (i) electrode material in ferroelectric memories having improved fatigue resistance, (ii) gate electrode for MOS transistors to overcome the depletion capacitance at polysilicium/SiO_2 interface, (iii) thin-film resistor with excellent temperature stability, (iv) diffusion barrier layer and interconnecting material in integrated circuits [4]. Recently, polycrystalline RuO_2 thin films were envisaged as promising electrodes, instead of classical metal platinum electrodes, for the fabrication of ferroelectric capacitor stacks (electrode/ferroelectric/electrode) to be used as dynamic random access memory (DRAM) and non-volatile random access memory (NVRAM) [3]. Platinum electrodes present a series of well known drawbacks: atomic diffusion through the Pt layer (diffusion of Si, oxygen and constituents of the ferroelectric film), electrical short-circuits of the capacitor due to the presence of hillocks on the Pt surface, poor adhesion of Pt on SiO_2, and a difficult etching process. Moreover, serious problems of fatigue and aging were encountered on the Pt/ferroelectric/Pt capacitors, leading to a reduction of the remnant polarization after about 10^8 cycles [5].

In the present work, we deal with a potential application of ferroelectric–catalytic thin layer associations, in the general

* Corresponding author. Tel.: +33 4 94 14 23 11; fax: +33 4 94 14 23 11.
E-mail address: gavarri.jr@univ-tln.fr (J.R. Gavarri).

0169-4332/$ – see front matter © 2007 Elsevier B.V. All rights reserved.
doi:10.1016/j.apsusc.2007.06.059

field of gas sensor technologies. Such ferroelectric–catalytic associations might present a double interest: (i) first, an improvement of multilayer chemical and mechanical stabilities, (ii) secondly, new application as piezoelectric–catalytic bilayers for surface acoustic wave devices.

As a first step, we have elaborated multilayer systems and studied the catalytic properties of RuO_2 films deposited on $SrBi_2Ta_2O_9$ (SBT) and $Ba_2NaNb_5O_{15}$ (BNN) ferroelectric films, in presence of methane gas. The SBT oxide presents a layered orthorhombic structure (with space group $A2_1am$ and cell parameters $a = 552.7$, $b = 553.7$, $c = 2499.1$ pm). The BNN oxide presents an orthorhombic structure (with space group Pba2, cell parameters $a = 1242$, $b = 1248$, $c = 397.7$ pm). In a later step, we should try to investigate the coupling of such catalytic interactions with electrical responses of these ferroelectric layers, in order to develop new gas sensor devices related to surface and bulk acoustic waves technologies.

RuO_2 films can be prepared via diversified chemical or physical routes: metal-organic chemical vapor deposition (MOCVD) [6], spray pyrolysis [7], sputtering [8,9], pulsed laser deposition (PLD) [10] and sol–gel approach [6] associated with spin coating process. In this work, RuO_2 films were deposited from sol gel and spin coating approaches, on three different substrates: (i) metal platinum deposited on silicium (Pt/Si), (ii) ferroelectric oxide SBT deposited on Si substrate (SBT/Si) and (iii) ferroelectric oxide BNN deposited on Si substrate (BNN/Si). The conversion of methane gas (in air–methane mixtures) was studied as a function of temperature, making use of homemade device and infrared spectroscopy.

2. Experimental

2.1. Preparation of solution

The following starting materials and reagents were used: ruthenium chloride ($RuCl_3$, xH_2O STREM CHEMICALS), absolute ethanol (C_2H_5OH). $RuCl_3$, xH_2O was dissolved in absolute ethanol with agitation. The obtained solution was maintained under agitation during 24 h. After 7 days of ageing, the solution was used for thin film preparation.

2.2. Films deposition

RuO_2 films were deposited using spin coating method. Before applying the sol–gel coating, substrates were washed in acetone and ethanol using an ultrasound bath during 1 h, rinsed with pure water and dried. All the substrates were washed except BNN/substrate. A unique spin coating process was applied to deposit RuO_2 precursor solution on Pt/Si, SBT/Si and BNN/Si substrates. The optimized spin coating parameters were as follows: rate of 4000 revolutions per min (rpm), acceleration of 2000 rpm/s, time of 15 s.

Classical commercial Pt/Si substrates (20 nm Pt deposited on Si) for microelectronics applications were used as standard initial substrates allowing comparing RuO_2 film behaviors, in presence of methane, as a function of diversified underlayers. Ferroelectric SBT film was deposited in a commercially available single-wafer reactor by metal-organic chemical vapor deposition. Ferroelectric BNN films were deposited by radio frequency magnetron sputtering making use of a specific equipment. Before RuO_2 deposition, BNN films were annealed at 400 °C during 1 h. After each deposition, each multilayer system was subsequently heated in a hotplate for 2 min, in order to evaporate solvents. This procedure was repeated several times until we obtained six layers of RuO_2 on the substrate. A final thermal treatment, aiming to promote stabilization and densification of the films and to remove unreacted organic residues, was carried out in a furnace at 450 °C for 2 h. The obtained films were characterized by X-ray diffraction (XRD) and scanning electron microscopy.

2.3. X-ray diffraction and scanning electron microscopy analyses

X-Ray Diffraction patterns were recorded on Siemens-Brucker D5000 equipment, with copper X-ray source ($\lambda = 154.06$ pm), Soller slides, a secondary monochromator. To analyze our thin films, it was necessary to use a grazing-incidence X-ray configuration, with an X-ray beam irradiating the thin film plane with a fixed α angle of 0.5°, a 2θ step of 0.05° and a counting time of 300 s.

Scanning electron microscopy (JEOL JSM- 5500) was used to characterize the surfaces of RuO_2 films deposited on the various substrates.

2.4. Fourier transform infrared spectroscopy (FTIR) and catalysis

The thin films were cut in identical forms, with similar apparent surfaces of 1 ± 0.1 cm^2. A homemade device coupling a specific reactor with FTIR spectrometer was used to study the catalytic efficiency of these systems [RuO_2 /ferroelectrics/Si] in presence of air–CH_4 mixture [11,12]. The catalytic efficiency is relative to the proportion of CO_2 (and H_2O) resulting from classical reaction: $CH_4 + O_2 \rightarrow CO_2 + H_2O$. The reactor was constituted of a cylindrical cell in which the sample could be subjected to reactive air–methane flow. The cell was heated in a furnace at temperatures ranging between room temperature and 450 °C. Preliminary studies of initial thin films, before any RuO_2 deposition, were carried out at varying temperatures to determine background analyses. Fig. 1 represents the reactor. The emitted gases resulting from conversion of methane into CO_2 and H_2O

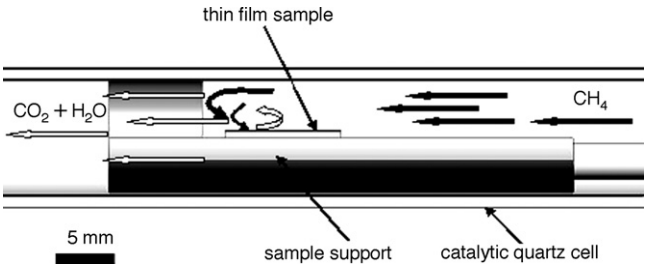

Fig. 1. Catalytic cell for gas solid interaction: air methane flow interacting with thin film.

were then led up to a FTIR spectrometer (UNICAM-MATTSON) allowing analyzing the intensity variations of vibration adsorption bands of CH_4, CO_2 and H_2O molecules. The intensities of these bands (surfaces of peaks) were assumed to directly give the conversion rates.

The gas flow-rate was constant (flow rate: 10 cm^3/mn; gas composition: 12,700 ppm CH_4 in air). The catalytic conversion was analyzed at various fixed temperatures (T = 100, 200, 250, 300, 350, 400 and 450 °C). For a given temperature, ninety FTIR spectra were recorded during 1 h, in order to observe time dependent fluctuations of conversion. The FTIR records were then statistically treated to give one unique average for each temperature.

3. Results and discussion

3.1. Structural and microstructural characterizations

Due to the small amounts of analyzed phases in thin films, XRD data only allowed identification of phases and evaluation of cell parameters. The RuO_2 phase was easily identified in each sample. The BNN phase was observed only as traces because of weak thickness of the BNN layer. In the case of RuO_2/SBT sample, all phases were clearly identified. As expected from the XRD configuration (grazing incidence) used in our analyses, Bragg peaks of silicium substrate were not observed. We report the XRD pattern of RuO_2/SBT sample on Fig. 2. Bragg peaks of RuO_2 and SBT phases are visible. Despite strong experimental errors due to the analysis, estimated elemental cell parameters were found in good agreement with standard parameters (see Section 1): RuO_2, a = 451, c = 311 pm; SBT, a = 553, b = 554, c = 2500 pm; BNN, a = 1242, b = 1248, c = 398 pm.

A microstructural study was performed by scanning electron microscopy (SEM). Scanning electron microscopy images (secondary electrons) of Fig. 3 (a–f) successively represent typical surfaces of RuO_2 deposited on Pt, SBT, BNN layers with various magnifications. Fig. 3 (a and b) show the surface morphology of RuO_2/Pt samples, after thermal treatment. The surface is uniform: a continuous layer of small grains having dimensions ranging between 0.5 and 1 μm is observable. Small white particles with dimensions of 1–5 μm are also observed on the surface. Fig. 3 (c and d) show the surface of RuO_2 deposited on SBT layer, after thermal treatment. The surface is homogeneous and formed of small grains (0.1–0.5 μm). Fig. 3 (e and f) represent the surface of RuO_2/BNN sample: grain linear dimensions also range from 0.1 to 0.5 μm, frequent discontinuities (cracks) having 5–30 μm of length are clearly observed. These large cracks in RuO_2 films probably result from a difference in adhesion of initial liquid solution deposited on BNN film during spin coating process. It should also be recalled that BNN film was deposited by RF sputtering technique, while SBT film was obtained from MOCVD. Such extended heterogeneities are generally undesirable in applications requiring continuous films and high adhesion: however, in our case, these imperfections associated with surface roughness might be interesting to improve CH_4 gas adsorption and catalytic efficiency.

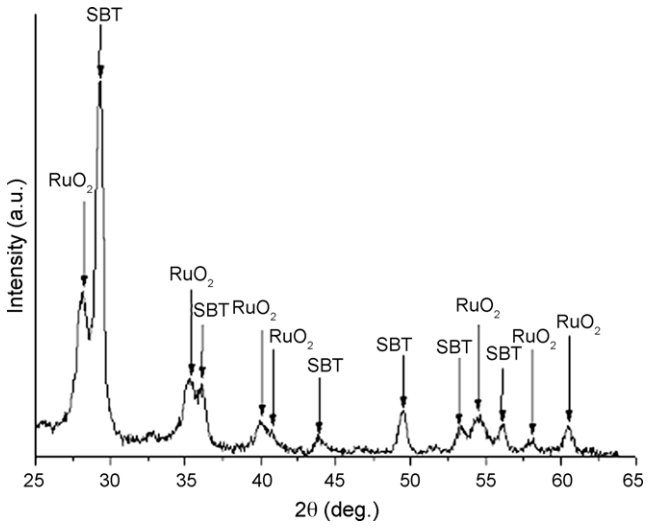

Fig. 2. XRD patterns of RuO_2/SBT/substrate after heating at 450 °C/2 h. Presence of RuO_2 and SBT phases.

3.2. FTIR analysis of catalytic efficiency

The initial SBT and BNN layers deposited on Si substrates (before any RuO_2 deposition) delivered no FTIR CO_2 signals when they were subjected to catalytic action of air methane flow. A specific FTIR analysis of the initial Pt/Si substrate, before any RuO_2 deposition, was carried out with the same air–methane flows corresponding to 12,000 ppm of CH_4. No catalytic response was evidenced in the temperature range 100–450 °C. Despite the well-known catalytic effect of Pt, this absence of conversion into CO_2 might be due to the very small amount of Pt on Si substrate (layer of 20 nm) and to the weak Pt specific active surface.

The typical absorption bands of CH_4, CO_2 and H_2O molecules are shown in Fig. 4 (a–c, respectively) for thermally treated RuO_2 on Pt (4a), SBT (4b) and BNN (4c) substrates. The evolution of the CO_2 peak surface can give a relative estimation of conversion rate and catalytic efficiency. In fact, the ratio CO_2 over CH_4 peaks surfaces should better represent the conversion efficiency. All surface measurements were normalized to the CH_4 band surface. Table 1 reports the numerical values of FTIR CO_2 band intensities due to catalytic conversion by each film,

Table 1
Conversion of CH_4 into CO_2

Temperature (°C)	I (RuO_2/Pt/Si)	I (RuO_2/SBT/Si)	I (RuO_2/BNN/Si)
100	0	0	0
200	0.078	0	0.122
250	0.156	0.18	0.427
300	0.702	0.765	0.732
350	0.975	2.025	1.281
400	2.535	2.52	3.355
450	2.613	2.61	3.721

Intensity (I) of CO_2 vibrational bands from FTIR analyses (in arbitrary units). I(RuO2/Pt, SBT, BNN): responses of RuO_2 on Pt, SBT, BNN layers.

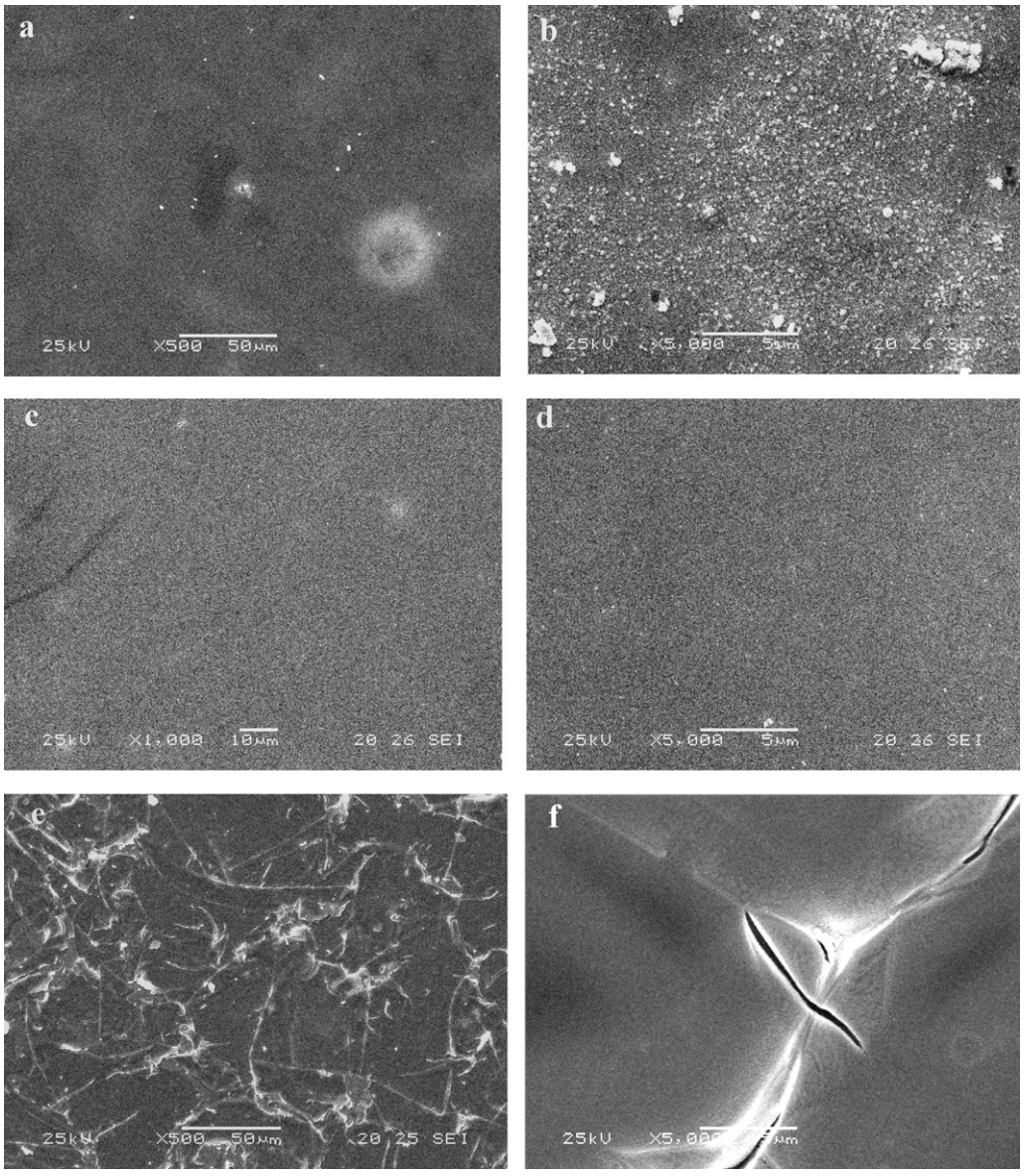

Fig. 3. Scanning Electron Microscopy images of RuO_2 films on Pt, SBT, BNN layers, with various magnifications: (a) Pt (×500), (b) Pt (×5000), (c) SBT (×1000), (d) SBT (×5000), (e) BNN (×500), (f) BNN (×5000). (b) Particles on RuO_2/Pt surface, (d) homogeneous RuO_2/SBT surface, (e and f) large defects and cracks on RuO_2/BNN surface.

for seven temperatures 100, 200, 250, 300, 350, 400 and 450 °C. These data were obtained after subtracting the residual CO_2 background, systematically observed at low temperatures in such experimental configuration, because of environmental conditions.

Fig. 5 reports these results. Let us recall that on abscissa (temperature axis), we have reported averaged data for a given temperature. The thermal evolution shows increasing catalytic activation up to an optimal temperature that we established as being close to 400 °C for RuO_2 catalyst. At low temperature, no significant conversion occurred, despite the fact that residual environmental CO_2 traces were observed. From 200 to 250 °C, CH_4 conversion into CO_2 started. Above 400 °C, catalytic efficiency was not improved in a significant way. The experiment at 450 °C shows that catalytic activation reached a limit.

The observed thermal evolution of catalytic activity can be interpreted in terms of elemental Arrhenius model as follows: $I(CO_2) = A\ \exp(-E/RT)$, where E is activation energy of catalytic mechanism for each sample. As a first approximation, we have obtained, for the Pt, SBT and BNN based samples, the following activation energies in $J\,mol^{-1}$: 43,295; 42,705; 39,190. In other terms, we observe a decreasing energetic barrier respectively for Pt, SBT and BNN based multilayers, which agrees well with a better capacity of BNN based samples to convert CH_4 into CO_2.

The main difficulty of such measurements resides in the fact that our system presents some fluctuations in flow rate, in catalytic interactions between gas and film, mainly because of gas convection occurring in the reactor cell. Other fluctuations might be caused by gas circulation in the spectrometer, and during evacuation of this gas out of the spectrometer. It is the

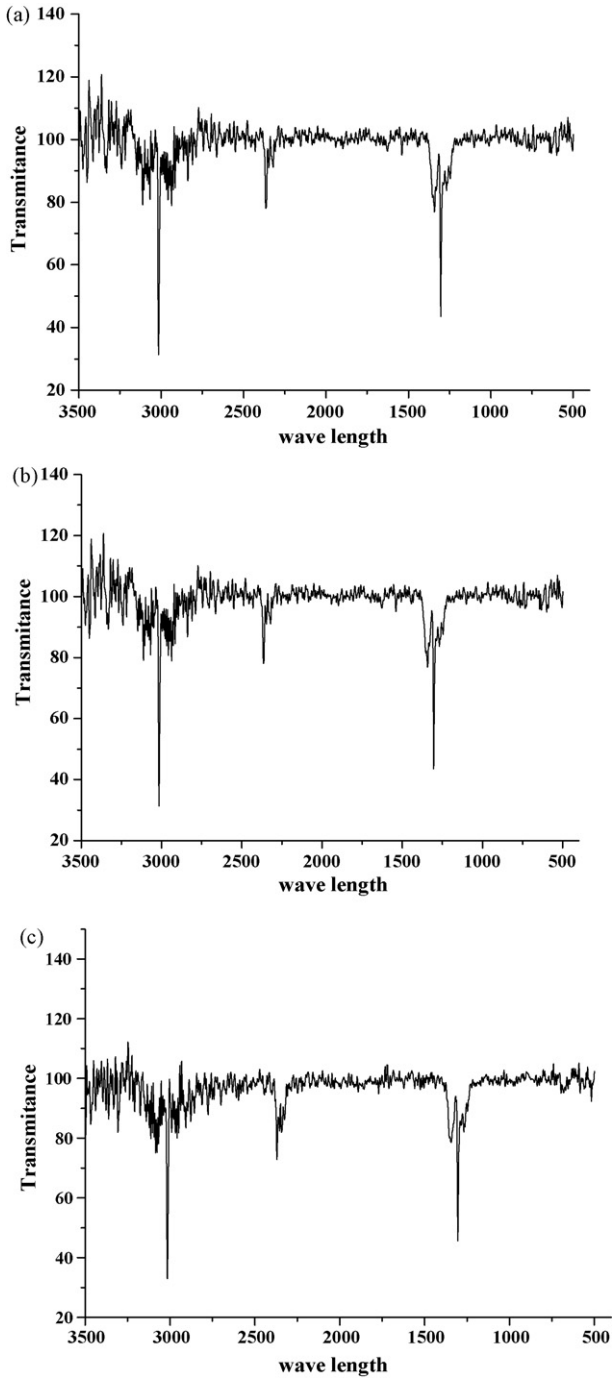

Fig. 4. (a) FTIR spectra obtained for RuO_2/Pt sample at 400 °C. FTIR Modes: CH_4, 3020 cm^{-1}; CO_2, 2350 cm^{-1}; H_2O, 1600 cm^{-1}. (b) FTIR spectra obtained for RuO_2/SBT sample at 400 °C. FTIR Modes: CH_4, 3020 cm^{-1}; CO_2, 2350 cm^{-1}; H_2O, 1600 cm^{-1}. (c) FTIR spectra obtained for RuO_2/BNN sample at 400 °C. FTIR Modes: CH_4, 3020 cm^{-1}; CO_2, 2350 cm^{-1}; H_2O, 1600 cm^{-1}.

reason why FTIR data were recorded during delays of 1 h for each fixed temperature. Finally, the general relative incertitude on I/I_0 values was estimated to be close to $\Delta \mathrm{Ln}\, I/I_0 = 0.10$ at 400 °C. This incertitude increases with decreasing catalytic temperature (I (CO_2) decreases). Despite these experimental incertitudes, we might admit that the catalytic efficiency of RuO_2/BNN samples was higher than that of the two other samples.

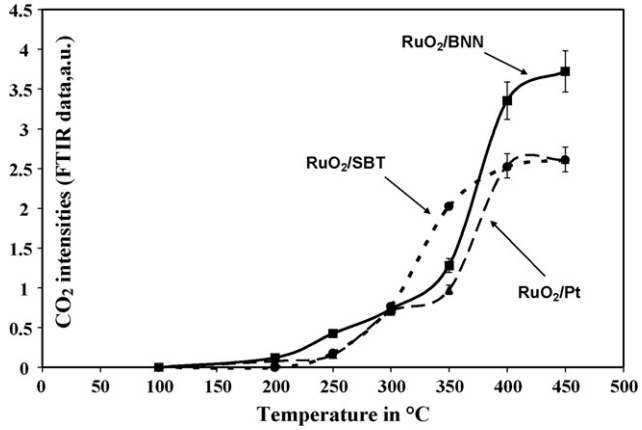

Fig. 5. Catalytic efficiency of RuO_2 films from FTIR data. CO_2 intensities of adsorption bands in arbitrary units: ▬, BNN; - - -, SBT; – – –, Pt. Data are obtained from statistical analysis of CO_2 intensity during 1 h at a fixed temperature.

These differences in catalytic behaviors might be interpreted in terms of surface roughness of RuO_2 film and / or coupling effect of Pt, SBT, BNN interlayers. In the case of Pt substrate, a good adhesion of initial RuO_2 precursor on Pt film should have allowed a homogeneous growth of RuO_2 film, giving rise to a relatively smooth surface, which is not in favor of optimal catalysis. In the case of SBT film deposited from MOCVD technique, the adhesion should also be satisfactory, probably because of the SBT surface nature. In addition, the crystal growth of RuO_2 on SBT should have been facilitated probably because of the oxide nature itself. In the case of BNN substrate, the deposition process was fully different (RF sputtering), and probably because of nature of BNN surface, adhesion of initial precursor film should have been insufficient, and cracks were generated during crystal growth and thermal treatment.

This difference in catalytic behavior might also be interpreted in terms of a hypothetical coupling of BNN with metallic RuO_2: in fact, cracks and porosity should facilitate interactions of CH_4 gas molecules with BNN/RuO_2 interfaces, improving gas adsorption along BNN/RuO2 corners, enhancing electron–oxygen exchanges at these interfaces.

4. Conclusion

In the present work, catalytic multilayers involving RuO_2 catalyst deposited on ferroelectric films were successfully synthesized. The various phases constituting catalyst and ferroelectrics were unambiguously identified from X-ray diffraction. SEM analyses allowed characterizing the surface qualities. Making use of a homemade device, FTIR analyses of CH_4/RuO_2 catalytic interactions under air–methane flows were performed at variable temperatures up to 450 °C. The RuO_2/SBT and RuO_2/BNN multilayers presented interesting catalytic efficiencies that appeared as being significantly improved in comparison with that of the RuO_2/Pt multilayer. These differences in catalytic activities might be due first to the two different deposition processes of ferroelectric layers, and secondly to the nature of adhesion between each Pt, SBT, or

BNN film and the RuO_2 layer. The observed performances of RuO_2/BNN multilayer might be connected with increased specific surface coupled with enhanced catalytic actions due to BNN/RuO_2 interfaces. Now, electrical measurements are planned in order to test these catalytic–ferroelectric multilayers and to better understand the influence of ferroelectric undercoating on catalytic responses.

References

[1] K. Takemura, T. Sakuma, Y. Miyasaka, Appl. Phys. Lett. 64 (1994) 2967.
[2] K.M. Glassford, J.R. Chelikowsky, Phys. Rev. B47 (1993) 1732.
[3] Emil.V. Jelenkovic, K.Y. Tong, W.Y. Cheung, S.P. Wong, Microelectron. Reliab. 43 (2003) 49–55.
[4] M. Wittmer, J. Vac. Sci. Technol. A2 (1984) 273.
[5] S.D. Bernstein, T.Y. Wong, Y. Kisler, R.W. Tustison, J. Mater. Res. 8 (1993) 12.
[6] Y.S. Huang, P.C. Liao, Sol. Energy Mater. Sol. Cells 55 (1998) 179.
[7] P.S. Patil, E.A. Ennaoui, C.D. Lokhande, M. Muller, M. Giersig, K. Diesner, H. Tributsch, Thin Solid Films 310 (1997) 57.
[8] L.-J. Meng, E. Fortunato, R. Nunos, M.P. dos Santos, J. Korean Phys. Soc. 32 (1998) S1835.
[9] J.G. Lee, Y.T. Kim, S.K. Min, J. Appl. Phys. 77 (1995) 5473.
[10] Q.X. Jia, S.G. Song, et al. Appl. Phys. Lett. 68 (1996) 1069.
[11] S. Saitzek, S. Villain, J.-R. Gavarri, Advanced Materials and Technologies, Material Science Forum, vol. 513, Trans Tech Publications, 2006, pp. 1–14.
[12] P. Nowakowski, S. Villain, J.-R. Gavarri, A. Kopia, J. Kusinski, Materials Engineering, Proceedings Advanced Materials Technologies AMT'2007, Warsaw, 17–21 June, 2007.